



# CFD Modelling and Simulation of the Thermal Management in a Polymer Electrolyte Membrane (PEM) Fuel Cell Stack

Kaoutar Kabouchi<sup>1,\*</sup>, Mohamed Karim Ettouhami<sup>1</sup>

<sup>1</sup> Equipe de modélisation des structures et systèmes mécaniques, Mohammed V University in Rabat, ENSAM, Rabat, Morocco

## ARTICLE INFO

### Article history:

Received 2 August 2024  
Received in revised form 1 September 2024  
Accepted 9 October 2024  
Available online 30 November 2024

### Keywords:

PEM fuel cell stack; COMSOL  
Multiphysics; Temperature distribution;  
Electric potential; Water activity

## ABSTRACT

Polymer Electrolyte Membrane fuel cells are a promising technology for clean energy conversion due to their high efficiency and low emissions. However, one of the critical challenges in the operation of fuel cells is the effective management of temperature and humidity within the fuel cell stack. Uneven temperature distribution can cause uneven water vapor condensation, leading to performance inconsistencies among individual cells in the stack. This necessitates a comprehensive understanding and control of the thermal and humidity dynamics within the fuel cell stack to ensure optimal performance and longevity. In this study, with the use of COMSOL Multiphysics, a mathematical polymer exchange membrane fuel cell stack model is designed and is applied to assess the thermal control of a stack of polymer exchange membrane fuel cell made up of two end plates, five membranes electrode assembly, and five cells. The boundary conditions are established and the mathematical equations are numerically solved. The obtained results indicate that the thermal and electrochemical performance within the fuel cell stack is significantly influenced by the distribution of cooling flow and gas reactants. It is found that higher temperatures near the outlet highlight the importance of optimizing cooling strategies to prevent overheating and ensure uniform temperature distribution. Moreover, the variations in relative humidity observed highlight the importance of effective water management, particularly in the first and last cells, to prevent flooding. This study also reveals the intricate relationship between temperature, humidity, and gas flow, which must be carefully balanced to prevent performance degradation. These insights suggest that optimizing the thermal and humidity management strategies is crucial for improving the durability and reliability of polymer exchange membrane fuel cell stacks.

## 1. Introduction

Fuel cells represent a promising technology for clean energy production, offering high efficiency and low environmental impact compared to conventional combustion-based power generation methods [1-6]. Among various types of fuel cells, Polymer Electrolyte Membrane (PEM) fuel cells stand out due to their efficiency, compact size, and versatility in applications ranging from automotive to stationary power generation [7,8].

\* Corresponding author.

E-mail address: [kaoutar\\_kabouchi@um5.ac.ma](mailto:kaoutar_kabouchi@um5.ac.ma) (Kaoutar Kabouchi)

<https://doi.org/10.37934/arnht.27.1.113>

Fuel cells are electrochemical devices that convert chemical energy directly into electrical energy through the reaction of fuel and oxidant [9-11]. They offer a clean and efficient alternative to conventional combustion-based power generation systems [12]. Common types include Proton Exchange Membrane (PEM), Solid Oxide Fuel Cells (SOFCs), and Molten Carbonate Fuel Cells (MCFCs), each with distinct operational characteristics and applications [13]. PEM fuel cells, in particular, are renowned for their high-power density, low operating temperature, and suitability for mobile and stationary applications [14,15].

A PEMFC stack consists of multiple individual PEMFCs electrically connected in series and parallel to achieve the desired voltage and current outputs [16-18]. Each cell comprises a proton-conducting polymer electrolyte membrane, typically made of perfluoro sulfonic acid material, sandwiched between an anode and a cathode. Hydrogen H<sub>2</sub> fuel is supplied to the anode, where it undergoes electrochemical oxidation to produce protons H<sup>+</sup> and electrons e<sup>-</sup> [19]. The H<sup>+</sup> migrate through the membrane to the cathode, where they combine with oxygen O<sub>2</sub> (from air) and e<sup>-</sup> to form water and release electrical energy [20]. The efficient operation of PEMFC stacks depends on effective water and heat management to maintain optimal performance and durability [21].

Computational Fluid Dynamics (CFD) simulation is indispensable in the development and optimization of PEMFC stacks [22-24]. It enables detailed analysis and visualization of fluid flow, heat transfer, and mass transport phenomena within the cells and across the stack [25]. By simulating complex interactions between fluid dynamics, electrochemical processes, and heat transfer, CFD helps engineers and researchers optimize stack design, improve thermal management strategies, and predict performance under varying operating conditions [26]. This predictive capability accelerates innovation in fuel cell technology, facilitating the design of more efficient and reliable PEM fuel cell stacks for diverse applications [27,28].

Research on the simulation and modeling of PEMFC stacks has been discussed in several papers. Choe and Shan [29] developed a dynamic PEMFC stack model, demonstrating uneven temperature distributions that varied continuously with operating loads and conditions. Kvesic *et al.*, [30] developed a CFD model for a short stack of five cells using a multi-scale and multi-domain approach, although they did not incorporate electrochemical equations, focusing instead on achieving the desired pressure drop. Mustata *et al.*, [31] investigated a 300 W stack's 3D model with two distinct gas inlets, solving the primary collectors and plate channels' Navier-Stokes equations. Their results provided a detailed spatial explanation of the pressure and flow fields. Mayyas *et al.*, [32] designed a 3D thermal model for estimating the thermal performance of air-cooled PEMFCs, demonstrating the model's capability to accurately predict thermal behavior under controlled conditions. Liu *et al.*, [33] presented a 3D model for an air-cooled mini fuel cell stack consisting of six cells with an active area of 8 cm<sup>2</sup>, simplifying the flow fields to porous media.

The study in the thermal management of the PEMFC stack is highly beneficial in optimizing performance, improving efficiency, and extending the lifespan of the fuel cell system.

In the present study, a three-dimensional mathematical model is developed to simulate and evaluate the thermal management within the PEMFC stack and analyze various parameters, including electric potential of the cell, hydrogen molar fraction distribution, oxygen molar fraction distribution, temperature distribution of the cell, temperature distribution in the MEAs, temperature distribution for various average cell voltages and water activity in the oxygen gas diffusion electrodes.

The paper is organized as follows: In Section 2, a comprehensive explanation of the model developed in this study is provided, including the governing equations and computational framework. Section 3 exhibits the implementation of our 3D PEMFC stack model using COMSOL Multiphysics. The obtained results of our investigation, along with a detailed analysis of the influence of various

parameters on the fuel cell stack performance are presented and discussed in Section 4. Finally, Section 5 concludes the study by summarizing the key findings.

## 2. Mathematical Modelling

### 2.1 Geometric Model

Figure 1 illustrates the repetitive unit cell used to create the model geometry. The bipolar plate (BPP), made from patterned steel sheets, separates the hydrogen and oxygen (air) gas compartments and includes a separate flow compartment for the cooling liquid. The BPP also features inlet and outlet manifolds that direct fluids to larger flow channels located outside the model geometry. This study's stack design utilizes a "Z" pattern for the gas flow channels, with the direction of the air channels shown in Figure 1. On the hydrogen side, the same pattern is used but mirrored in the yz-plane. For the cooling flow, a uniform direction along the y-axis is assumed. Membrane-electrode assemblies (MEAs), comprising one gas diffusion layer (GDL) and one gas diffusion electrode (GDE) per gas compartment, and a polymer electrolyte membrane in between, are placed between each BPP.

The cooling flow compartments are created by combining the hydrogen and oxygen sides of the BPPs when stacking the unit cells. Generally, in stack design, as a result of only having to provide flow of one gas, the first and end plates have to be designed differently compared to the inner plates. The larger arrows represent the direction of the flow channels within the oxygen (air) section of the bipolar plate.

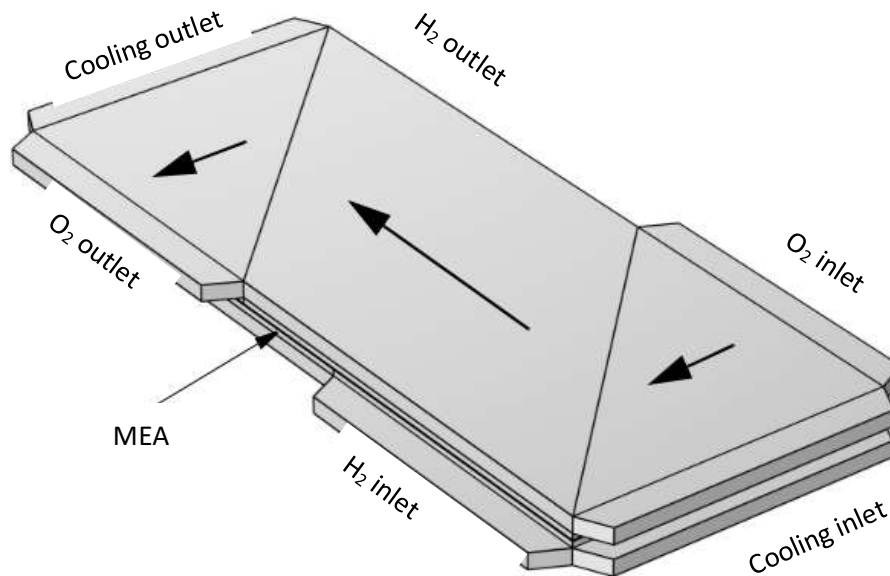
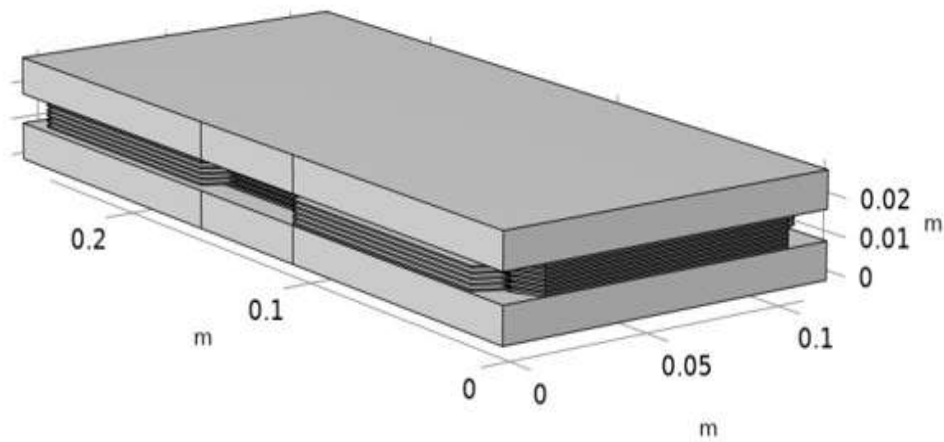


Fig. 1. Repetitive unit cell

The individual channels in the patterned BPPs are not explicitly resolved in the model geometry. Instead, the BPPs are divided into distinct domains aligned with the main gas flow direction. Homogenized flow equations based on Darcy's Law are then applied to define the flow, using anisotropic permeabilities corresponding to the channel directions.

The final design, depicted in Figure 2, consists of five-unit cells stacked together two end blocks, including front and end cooling "half" BPPs. Metal end blocks are added outside the stack for current conduction and structural rigidity. The assembly's geometry is completed with the boundary positioned at the center of the membranes, allowing for non-matching meshes on either side,

facilitating mesh sweeping in the through-plane direction. Table 1 reports the design parameters used in the developed model.



**Fig. 2.** Model geometry consisting of five-unit cells and two end blocks

**Table 1**

Design parameters

Description	Value
Active area length $L_{plate}$	0.24 m
Active area width $W_{plate}$	0.1 m
Manifold width $W_{manifold}$	0.09 m
Manifold length $L_{manifold}$	0.01 m
Current collector thickness $D_{cc}$	0.01 m
Bipolar plate thickness $D_{bpp}$	0.001 m
Gas diffusion layer thickness $D_{gdl}$	2 e-4 m
Membrane thickness $D_{mem}$	3 e-5 m
Unit cell thickness $D_{cell}$	0.00143 m
Number of cells $N_{cells}$	5

## 2.2 Basic Assumptions

The computational model was based on the following assumptions:

- i) Steady-state conditions,
- ii) Laminar flow within the channels,
- iii) Isotropic characteristics of porous zones,
- iv) Species transport occurring in the gas phase,
- v) All gases and water exist in a gaseous state,
- vi) Reaction gases behave as ideal gases,
- vii) Constant material parameters throughout,
- viii) No gas or water crossover through the membrane.

### 2.3 Governing Equations

The transport phenomena within the PEMFC stack are governed by the equations of charge transport, species, energy, momentum, and mass conservation [34-36]. These fundamental equations are shown below:

Continuity equation:

$$\nabla \cdot (\rho \vec{v}) = S_m \quad (1)$$

where  $S_m$  stands for the source term in the species balance equation,  $\vec{v}$  is the vector velocity and  $\rho$  represents the fluid density.

Momentum transport:

$$\nabla \cdot (\rho \vec{v} \vec{v}) = -\nabla p + \nabla \cdot (\mu^{eff} \nabla \vec{v}) + S_p \quad (2)$$

where  $S_p$  is a source term that encompasses the physical properties of the porous media,  $p$  represents the static pressure and  $\mu^{eff}$  denotes the effective viscosity of the mixture.

Species transport:

$$\nabla \cdot (\rho \vec{v} y_i) = -\nabla \cdot \vec{J}_i + S_i \quad (3)$$

where  $\vec{J}_i$  denotes the diffusion flux for species  $i$  and  $S_i$  represents the source term for each phase.

Energy:

$$\nabla \cdot [\vec{v} (\rho E + p)] = \nabla \cdot \left( k_{eff} \nabla T - \sum_i h_i \vec{J}_i \right) \quad (4)$$

where  $E$  is the total energy,  $\vec{J}_i$  is the diffusion flux for species  $i$ ,  $k_{eff}$  denotes the effective conductivity and  $E$  represents the total energy.

Electrochemical model:

$$\nabla \cdot (\sigma_{sol} \nabla \varphi_{sol}) + R_{sol} = 0 \quad (5)$$

$$\nabla \cdot (\sigma_{mem} \nabla \varphi_{mem}) + R_{mem} = 0 \quad (6)$$

where the subscripts 'mem' and 'sol' refer to the electrolyte phases and solid, respectively,  $\varphi$  is the potential of the cell and  $R$  stands for the transfer current and  $\sigma$  represents the electric or ionic conductivity.

## 2.4 Boundary Conditions

We established boundary conditions to accurately emulate the operational environment of the PEMFC stack. This involved the specification of operational parameters crucial for simulation, including temperature, pressure, and voltage. These parameters are pivotal in delineating the intricate thermal behaviour within the fuel cell system. In our baseline case, specific parameter values for the simulation are detailed in Section "Numerical Procedure." This delineation of boundary conditions ensures the fidelity of our computational model in accurately capturing the thermal dynamics and overall performance of the PEMFC stack.

## 3. Numerical Procedure

The triangular mesh is used to mesh the model's geometry (generate prisms) on the hydrogen and the oxygen Gas Diffusion Electrodes and a swept mesh on the membranes, the oxygen GDLs, the hydrogen GDLs, cooling channels and manifolds by COMSOL Multiphysics software (Figure 3). For this model, we used a user-defined mesh. The meshing process involves sweeping the mesh along the through-plane direction of the stack. There are 20500 elements of edge, 457118 elements of boundary, and 917024 elements of domain in the complete mesh. Boundary conditions from COMSOL were applied to solve the mathematical equations, and a methodology established on the method of finite elements was utilized. The model was operated at a cell voltage of 0.85 V. The physicochemical characteristics developed in this structure are reported in Table 2.

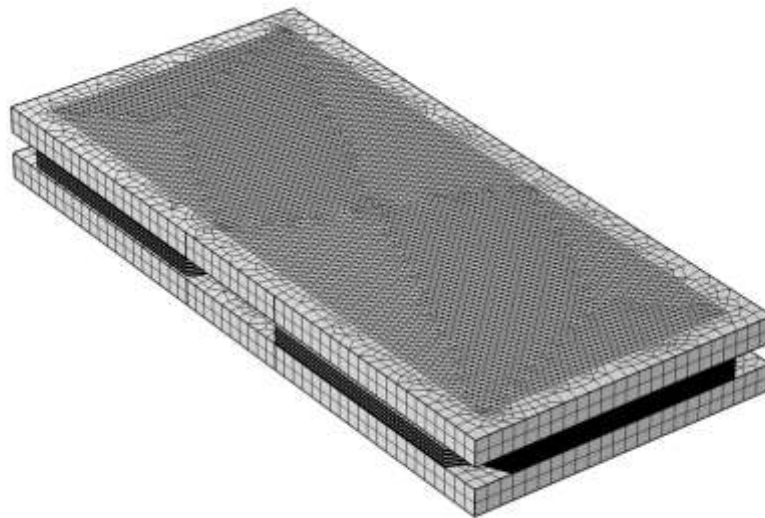


**Fig. 3.** Structure after meshing

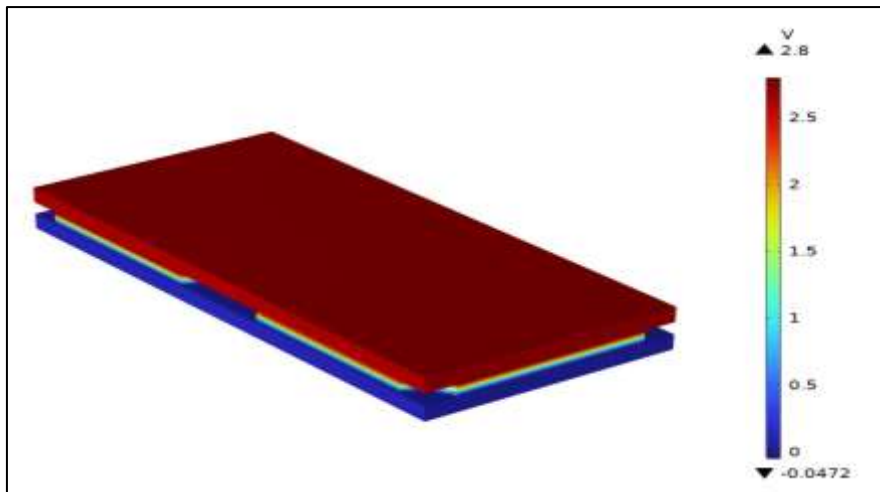
**Table 2**  
Physicochemical characteristics

Parameter	Value
GDL thru plane thermal conductivity	0.3 W/(m.K)
GDL in plane thermal conductivity	3 W/(m.K)
Effective thermal conductivity, bipolar plate	4.5 W/(m.K)
Average cell voltage	0.85 V
Stack voltage	4.25 V
Effective permeability, bipolar plate	5 e-9 m <sup>2</sup>
Exchange current density, H <sub>2</sub> oxidation	100 A/m <sup>2</sup>
Exchange current density, O <sub>2</sub> reduction	1 e-4 A/m <sup>2</sup>
Specific area, catalytic layers	5 e7 1/m
Electric conductivity, gas diffusion layers	200 S/m
Gas permeability, gas diffusion layers	5 e-12 m <sup>2</sup>
Anodic transfer coefficient, oxygen reduction	3
Gas phase volume fraction, gas diffusion layers	0.6
Solid phase volume fraction, gas diffusion layers	0.4
Catalytic layer thickness	1 e-5 m
Initial average cell voltage in auxiliary sweep	0.85 V
Inlet temperature	333.15 K
Inlet gas pressure, cathode side	8000 Pa
Inlet gas pressure, anode side	2000 Pa
Cooling liquid permeability, bipolar plate	1 e-8 m <sup>2</sup>
Gas volume fraction in bipolar plate	0.45
Cooling liquid volume fraction in bipolar plate	0.45
Effective electric conductivity, bipolar plate	1000 S/m
Cooling liquid inlet velocity	0.1 m/s
Stack thickness	0.02915 m

#### 4. Results and Discussions

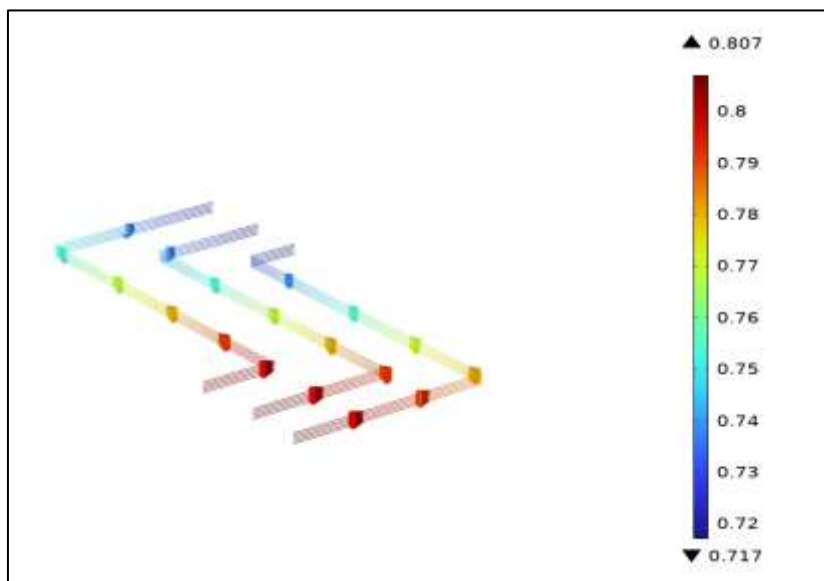
In this section, an evaluation of the performance of the PEMFC stack was carried out using COMSOL Multiphysics software. Main parameters, which include electric potential of the cell, hydrogen molar fraction distribution, oxygen molar fraction distribution, temperature distribution of the cell, temperature distribution in the MEAs, temperature distribution for various average cell voltages and water activity in the oxygen gas diffusion electrodes are shown in Figures 4-10.

In Figure 4, the electrode phase potential within the stack is depicted for an average cell voltage of 0.55 V. As we move from the red-colored upper side to the blue-colored bottom side of the stack, there is a significant decrease in potential.



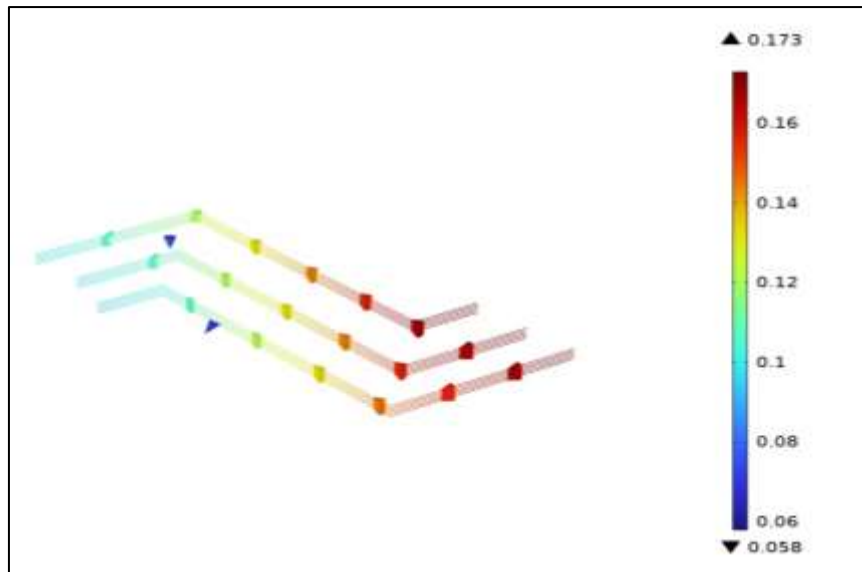
**Fig. 4.** Phase potential of the electrode for an average cell voltage of 0.55 V

Figure 5 depicts the streamlines of hydrogen flux with their respective molar fractions. Due to hydrogen consumption, the molar fraction decreases towards the outlet. Likewise, Figure 6 illustrates the streamlines of oxygen and their molar fractions within the air gas compartment. Depletion effects appear to be slightly more pronounced compared to those observed on the hydrogen side.



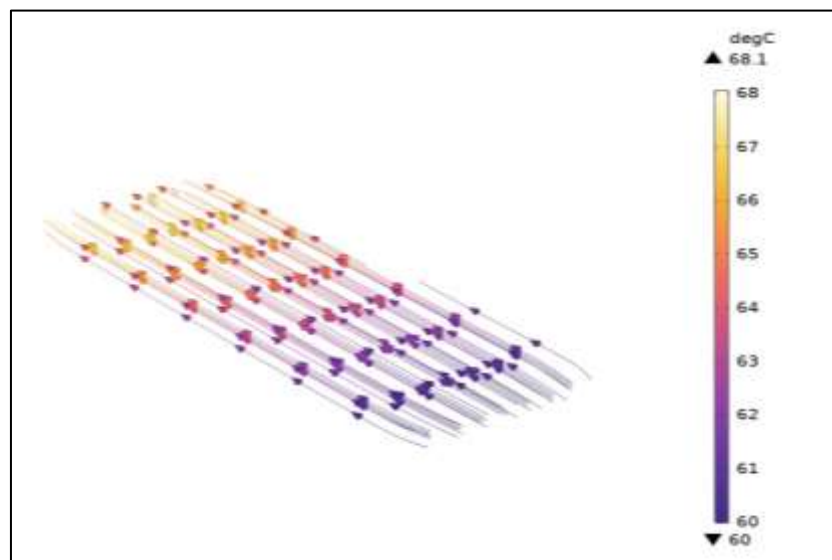
**Fig. 5.** Molar fraction (color legend) and molar flow (streamlines) of hydrogen for an average cell voltage of 0.55 V





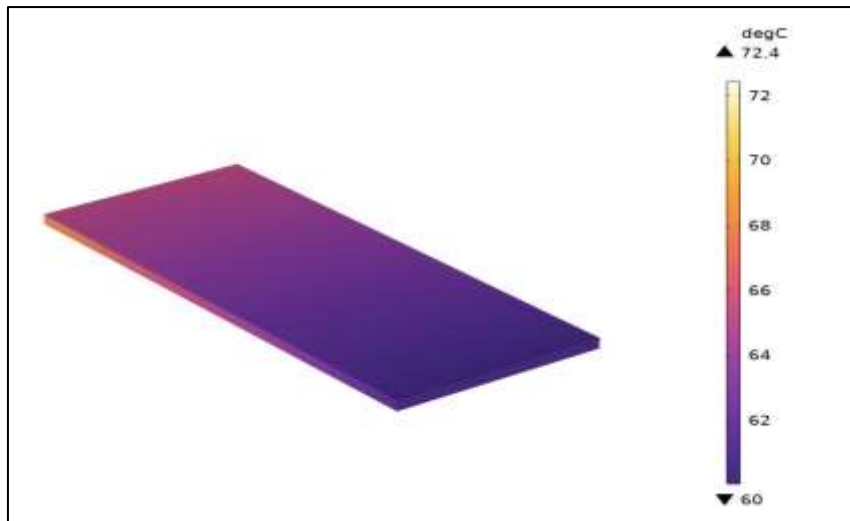
**Fig. 6.** Molar fraction (color legend) and molar flow (streamlines) of oxygen for an average cell voltage of 0.55 V

Figure 7 displays the flow streamlines of the cooling process with the associated temperature distribution, with temperatures progressively increasing towards the outlet. Our findings regarding temperature distribution within the PEM fuel cell stack are consistent with those of Shan and Choe [29], who also observed uneven temperature distribution at higher loads, reinforcing the importance of optimized cooling strategies. However, unlike Kvesic *et al.*, [30], who focused on the pressure drop and did not include electrochemical reactions in their model, our study integrates electrochemical and thermal aspects, providing a more holistic view of the stack's performance under operational conditions.



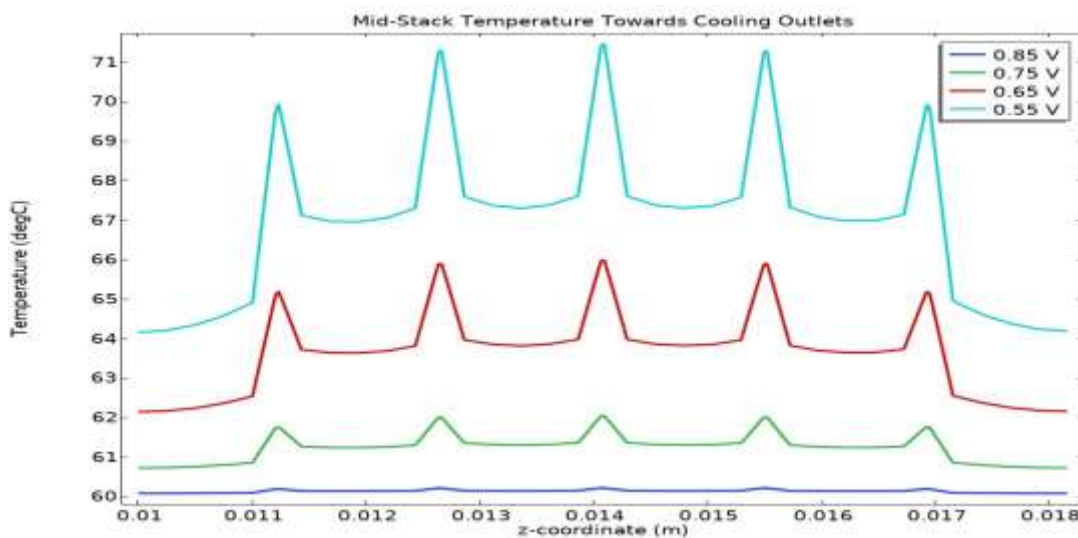
**Fig. 7.** Temperature stream lines (color legend) and cooling flow for an average cell voltage of 0.55 V

Figure 8 illustrates the temperature distribution within the MEAs, indicating an increased temperature gradient closer to the membrane.



**Fig. 8.** Distribution of the temperature in the MEAs for an average cell voltage of 0.55 V

Figure 9 provides additional insight into the temperature distribution across the stack in the through-plane direction. In this depiction, temperatures are charted along a line running in the z-axis, positioned at the center of the stack in the x-axis, and around 1 cm away from the outlet cooling manifold in the y-axis. It is evident that polarizing the stack leads to notable temperature variations within the MEA. Furthermore, we observe cooler temperatures in both the initial and final cells, attributable to these cells receiving a comparatively higher average cooling flow than the inner cells.



**Fig. 9.** Temperature for various average cell voltages along a z-directed line across the stack, near the outlet at half the cells width

Figure 10 depicts the water activity, or relative humidity, within the oxygen gas diffusion layer. Relative humidity is influenced by both water production and temperature. Typically, one would anticipate higher relative humidity towards the outlet due to water production in the cell. However, the higher temperature towards the outlet complicates this expectation, leading to a more intricate relationship, influenced by both cooling fluid distribution and the gas "Z"-flow field design.

It's worth noting that relative humidity levels tend to be higher in the first and last cells of the stack, primarily because of the generally lower temperatures in these cells. This suggests that these

cells are more prone to water flooding. To enhance stack design, one might consider adjusting the cooling flow patterns to mitigate cooling effects on the first and last cells. The variations in water activity across the cells, particularly near the first and last cells, indicate an interaction between temperature and humidity, as noted by Mustata *et al.*, [31]. However, our study advances this understanding by demonstrating how gas flow dynamics and cooling patterns influence water condensation and temperature gradients. These findings could be valuable in enhancing thermal management designs for future PEMFC systems.

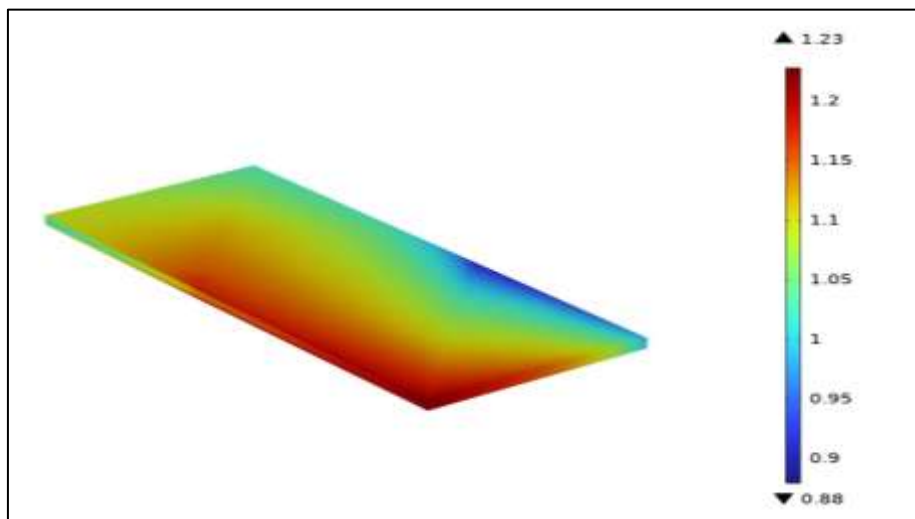


**Fig. 10.** Water activity in the oxygen gas diffusion electrodes for an average cell voltage of 0.55 V

## 5. Conclusions

In conclusion, a study utilizing the COMSOL Multiphysics software was executed to assess the PEMFC stack's thermal management. The stack consists of two end plates, five MEAs, and five cells. A three-dimensional model of the PEMFC stack was processed by thermal modelling to examine various parameters, including the electric potential of the cell, hydrogen and oxygen molar fraction distributions, temperature profiles across the cells and MEAs, and water activity in the oxygen gas diffusion electrodes. It is found that optimizing the distribution of cooling flow and gas reactants is crucial for maintaining uniform temperature and humidity levels within the stack. The higher temperatures observed near the outlet emphasize the need for efficient cooling strategies to prevent overheating and ensure consistent performance across all cells. Moreover, managing water vapour condensation and humidity levels, especially in the first and last cells, is essential to prevent flooding and maintain optimal operational conditions. These insights underscore the intricate interplay between temperature, humidity, and gas flow dynamics in PEM fuel cell stacks. While this study provides valuable insights into the thermal management of PEM fuel cell stacks, the model has certain limitations. The assumptions of steady-state conditions and ideal gas behavior might restrict the generalizability of the results, particularly under dynamic operational scenarios. Future research should focus on enhancing the model to include transient conditions, varying material properties, and more complex geometries to better replicate real-world conditions. Additionally, investigating the impact of these factors on long-term performance and degradation could offer more comprehensive guidance for optimizing PEM fuel cell designs.

## Acknowledgement

This research is funded by Mohammed V University in Rabat. The authors express their sincere gratitude for the support.

## References

- [1] Habib, Mohamed A., Gubran AQ Abdulrahman, Awad BS Alqaity, and Naef AA Qasem. "Hydrogen combustion, production, and applications: A review." *Alexandria Engineering Journal* 100 (2024): 182-207. <https://doi.org/10.1016/j.aej.2024.05.030>
- [2] Verma, Amit Kumar, Prerna Tripathi, Akhoury Sudhir Kumar Sinha, and Shikha Singh. "Advanced Materials in Energy Conversion Devices: Fuel Cells and Biofuel Cells." *Smart Materials for Science and Engineering* (2024): 269-285. <https://doi.org/10.1002/9781394186488.ch13>
- [3] Parthiban, D., D. Rajesh, Iyan Kumar, and K. Muninathan. "Performance Optimisation of Proton Exchange Membrane Fuel Cell by Modifying Anode Flow Field Design." *Advanced Energy Conversion Materials* (2024): 224-239. <https://doi.org/10.37256/aecm.5220244684>
- [4] Kabouchi, Kaoutar, Mohamed Karim Ettouhami, Hamid Mounir, and Khalid Elbikri. "Performance Investigation of PEM Fuel Cell with Three-Pass Serpentine Flow Fields under Varying Operating Voltages." *CFD Letters* 16, no. 10 (2024): 54-63. <https://doi.org/10.37934/cfdl.16.10.5463>
- [5] Rolo, Inês, Vítor AF Costa, and Francisco P. Brito. "Hydrogen-Based Energy Systems: Current Technology Development Status, Opportunities and Challenges." *Energies* 17, no. 1 (2023): 180. <https://doi.org/10.3390/en17010180>
- [6] Herlambang, Yusuf Dewantoro, Fatahul Arifin, Totok Prasetyo, and Anis Roihatin. "Numerical analysis of phenomena transport of a proton exchange membrane (PEM) fuel cell." *Journal of Advanced Research in Fluid Mechanics and Thermal Sciences* 80, no. 2 (2021): 127-135. <https://doi.org/10.37934/arfmts.80.2.127135>
- [7] Lindorfer, Johannes, Daniel Cenk Rosenfeld, and Hans Böhm. "Fuel cells: Energy conversion technology." In *Future energy*, pp. 495-517. Elsevier, 2020. <https://doi.org/10.1016/B978-0-08-102886-5.00023-2>
- [8] Sapkota, Prabal, Cyrille Boyer, Rukmi Dutta, Claudio Cazorla, and Kondo-Francois Aguey-Zinsou. "Planar polymer electrolyte membrane fuel cells: powering portable devices from hydrogen." *Sustainable Energy & Fuels* 4, no. 2 (2020): 439-468. <https://doi.org/10.1039/C9SE00861F>
- [9] Ragupathy, Pitchai, Santoshkumar Dattatray Bhat, and Nallathamby Kalaiselvi. "Electrochemical energy storage and conversion: An overview." *Wiley Interdisciplinary Reviews: Energy and Environment* 12, no. 2 (2023): e464. <https://doi.org/10.1002/wene.464>
- [10] Pramuanjaroenkij, Anchasa, and Sadik Kakaç. "The fuel cell electric vehicles: The highlight review." *International Journal of Hydrogen Energy* 48, no. 25 (2023): 9401-9425. <https://doi.org/10.1016/j.ijhydene.2022.11.103>
- [11] Zhang, Shidong, Steffen Hess, Holger Marschall, Uwe Reimer, Steven Beale, and Werner Lehnert. "openFuelCell2: A new computational tool for fuel cells, electrolyzers, and other electrochemical devices and processes." *Computer Physics Communications* 298 (2024): 109092. <https://doi.org/10.1016/j.cpc.2024.109092>
- [12] Dincer, Ibrahim, and Canan Acar. "A review on clean energy solutions for better sustainability." *International Journal of Energy Research* 39, no. 5 (2015): 585-606. <https://doi.org/10.1002/er.3329>
- [13] Giorgi, Leonardo, and Fabio Leccese. "Fuel cells: Technologies and applications." *The Open Fuel Cells Journal* 6, no. 1 (2013): 1-20. <https://doi.org/10.2174/1875932720130719001>
- [14] Aminudin, M. A., S. K. Kamarudin, B. H. Lim, E. H. Majilan, M. S. Masdar, and N. Shaari. "An overview: Current progress on hydrogen fuel cell vehicles." *International Journal of Hydrogen Energy* 48, no. 11 (2023): 4371-4388. <https://doi.org/10.1016/j.ijhydene.2022.10.156>
- [15] Kabouchi, Kaoutar, Mohamed Karim Ettouhami, and Hamid Mounir. "Simulation Examination of the Impact of Operating Parameters on a High-Temperature Proton Exchange Membrane Fuel Cell." *Mathematical Modelling of Engineering Problems* 11, no. 6 (2024). <https://doi.org/10.18280/mmep.110624>
- [16] Yakut, Yurdağül Benteşen. "A new control algorithm for increasing efficiency of PEM fuel cells–Based boost converter using PI controller with PSO method." *International Journal of Hydrogen Energy* 75, (2023): 1-11. <https://doi.org/10.1016/j.ijhydene.2023.12.008>
- [17] Arif, Muhammad, Sherman CP Cheung, and John Andrews. "Different approaches used for modeling and simulation of polymer electrolyte membrane fuel cells: A review." *Energy & Fuels* 34, no. 10 (2020): 11897-11915. <https://doi.org/10.1021/acs.energyfuels.0c02414>
- [18] Ferreira, Rui B., Diogo FM Santos, A. M. F. R. Pinto, and D. S. Falcão. "Development and testing of a PEM fuel cell stack envisioning unmanned aerial vehicles applications." *International Journal of Hydrogen Energy* 51 (2024): 1345-1353. <https://doi.org/10.1016/j.ijhydene.2023.05.090>

- [19] Mahato, Neelima, Hyeji Jang, Archana Dhyani, and Sunghun Cho. "Recent progress in conducting polymers for hydrogen storage and fuel cell applications." *Polymers* 12, no. 11 (2020): 2480. <https://doi.org/10.3390/polym12112480>
- [20] Wang, X. R., Y. Ma, J. Gao, T. Li, G. Z. Jiang, and Z. Y. Sun. "Review on water management methods for proton exchange membrane fuel cells." *International Journal of Hydrogen Energy* 46, no. 22 (2021): 12206-12229. <https://doi.org/10.1016/j.ijhydene.2020.06.211>
- [21] Madheswaran, Dinesh Kumar, Arunkumar Jayakumar, and Edwin Geo Varuvel. "Recent advancement on thermal management strategies in PEM fuel cell stack: a technical assessment from the context of fuel cell electric vehicle application." *Energy Sources, Part A: Recovery, Utilization, and Environmental Effects* 44, no. 2 (2022): 3100-3125. <https://doi.org/10.1080/15567036.2022.2058122>
- [22] Chen, Yong, Louise Enearu, Diogo Montalvão, and Thamo Sutharssan. "A Review of Computational Fluid Dynamics Simulations on PEFC Performance." *Journal of Applied Mechanical Engineering* (2016). <https://doi.org/10.4172/2168-9873.1000241>
- [23] Yu, Zeting, Lei Xia, Guoping Xu, Changjiang Wang, and Daohan Wang. "Improvement of the three-dimensional fine-mesh flow field of proton exchange membrane fuel cell (PEMFC) using CFD modeling, artificial neural network and genetic algorithm." *International Journal of Hydrogen Energy* 47, no. 82 (2022): 35038-35054. <https://doi.org/10.1016/j.ijhydene.2022.08.077>
- [24] Gopi, K. H., A. Nambi, and N. Rajalakshmi. "Design and development of open cathode PEM fuel cell–flow analysis optimization by CFD." *Fuel Cells* 20, no. 1 (2020): 33-39. <https://doi.org/10.1002/fuce.201900124>
- [25] Sarjuni, C. A., B. H. Lim, E. H. Majlan, and M. I. Rosli. "A review: Fluid dynamic and mass transport behaviour in a proton exchange membrane fuel cell stack." *Renewable and Sustainable Energy Reviews* 193 (2024): 114292. <https://doi.org/10.1016/j.rser.2024.114292>
- [26] Kim, Youchan, Kisung Lim, Hassan Salihi, Seongku Heo, and Hunchul Ju. "The Effects of Stack Configurations on the Thermal Management Capabilities of Solid Oxide Electrolysis Cells." *Energies* 17, no. 1 (2023): 125. <https://doi.org/10.3390/en17010125>
- [27] Zhang, Caizhi, Yuqi Zhang, Lei Wang, Xiaozhi Deng, Yang Liu, and Jiujun Zhang. "A health management review of proton exchange membrane fuel cell for electric vehicles: Failure mechanisms, diagnosis techniques and mitigation measures." *Renewable and Sustainable Energy Reviews* 182 (2023): 113369. <https://doi.org/10.1016/j.rser.2023.113369>
- [28] Wang, Junye. "Barriers of scaling-up fuel cells: Cost, durability and reliability." *Energy* 80, (2015): 509-521. <https://doi.org/10.1016/j.energy.2014.12.007>
- [29] Shan, Yuyao, and Song-Yul Choe. "Modeling and simulation of a PEM fuel cell stack considering temperature effects." *Journal of Power Sources* 158, no. 1 (2006): 274-286. <https://doi.org/10.1016/j.jpowsour.2005.09.053>
- [30] Kvesić, Mirko, Uwe Reimer, Dieter Froning, Lukas Lüke, Werner Lehnert, and Detlef Stolten. "3D modeling of a 200 cm<sup>2</sup> HT-PEFC short stack." *International journal of hydrogen energy* 37, no. 3 (2012): 2430-2439. <https://doi.org/10.1016/j.ijhydene.2011.10.055>
- [31] Mustata, Radu, Luis Valino, Félix Barreras, María Isabel Gil, and Antonio Lozano. "Study of the distribution of air flow in a proton exchange membrane fuel cell stack." *Journal of Power Sources* 192, no. 1 (2009): 185-189. <https://doi.org/10.1016/j.jpowsour.2008.12.083>
- [32] Mayyas, Abdel Raouf, Dilip Ramani, Arunachala M. Kannan, Keng Hsu, Ahmad Mayyas, and Tony Schwenn. "Cooling strategy for effective automotive power trains: 3D thermal modeling and multi-faceted approach for integrating thermoelectric modules into proton exchange membrane fuel cell stack." *International journal of hydrogen energy* 39, no. 30 (2014): 17327-17335. <https://doi.org/10.1016/j.ijhydene.2014.08.034>
- [33] Liu, Zhixiang, Zongqiang Mao, Cheng Wang, Weilin Zhuge, and Yangjun Zhang. "Numerical simulation of a mini PEMFC stack." *Journal of Power Sources* 160, no. 2 (2006): 1111-1121. <https://doi.org/10.1016/j.jpowsour.2006.03.001>
- [34] Kabouchi, Kaoutar, Mohamed Karim Ettouhami, and Hamid Mounir. "Computational Modeling of the Thermal Behavior in Passive Proton Exchange Membrane Fuel Cell." In *2024 4th International Conference on Innovative Research in Applied Science, Engineering and Technology (IRASET)*, pp. 1-6. IEEE, 2024. <https://doi.org/10.1109/IRASET60544.2024.10549619>
- [35] Sierra, J. M., S. J. Figueroa-Ramírez, S. E. Díaz, J. Vargas, and P. J. Sebastian. "Numerical evaluation of a PEM fuel cell with conventional flow fields adapted to tubular plates." *International journal of hydrogen energy* 39, no. 29 (2014): 16694-16705. <https://doi.org/10.1016/j.ijhydene.2014.04.078>
- [36] Macedo-Valencia, J., J. M. Sierra, S. J. Figueroa-Ramírez, S. E. Díaz, and M. Meza. "3D CFD modeling of a PEM fuel cell stack." *International journal of hydrogen energy* 41, no. 48 (2016): 23425-23433. <https://doi.org/10.1016/j.ijhydene.2016.10.065>